Matter
Previews

CellPress

Structural visualization of ultrathin chiral porous metal-organic framework nanosheet

Yin Zhang,[1] Pui Ching Lan,[1] and Shengqian Ma[1,*]

In the recent work of Cui et al., the design, preparation, and characterization of ultrathin chiral metal-organic frameworks nanosheets (MONs) have been thoroughly investigated, which expands the foundation for this field.

Porous crystalline metal-organic frameworks (MOFs) have drawn much attention for their broad applications in catalysis, separation, and sensing.[1] Likewise, exhibiting larger surface area, increasing number of unsaturated coordination centers and accessible active sites, and improving confinement effects, metal-organic frameworks nanosheets (MONs) are advantageous over their bulk counterparts, and such distinct physicochemical properties highlight their role in achieving superior performance. Generally, there are two methods to prepare MONs—the top-down method based on balling[2] and sonication exfoliation[3] of bulk MOFs, and the bottom-up method, which restricts the overgrowth of crystal in the vertical dimension via interfacial growth,[4] the Langmuir-Blodgett technique,[5] and molecule-[6] or ion-assisted route.[7] Noteworthily, the production of chiral MONs for high-demanding chirality-related areas is of greater interest but lacks strategy. Unlike achiral MOFs built from symmetric ligands such as terephthalic acid and porphyrin derivatives, which are easier for MON preparation, chiral MOFs with the asymmetric character have to be constructed from strong metal-ligand coordination bonding, leading to their weak electronic irradiation sensitivity and intrinsic structural fragility, which makes it difficult to obtain chiral MONs through delamination or confinement growth and high-resolution transmission electron microscope (TEM) image. Until now, only scarce works have been reported in regard to chiral MON preparation. In 2018, Tang's group provided their solution via a bottom-up inverse microemulsion (dioctylsulfosuccinate sodium [NaAOT]/isooctane) method in which metal-organic chains assemble into layers within microemulsion with the aid of strong hydrogen bonding and grow into two-dimensional MOFs of few layers under such a confined environment via weak hydrogen bonding and hydrophobic interaction.[8] Obviously, the rationality lies in mediating proper coordination mode and interaction by the design of chiral ligand and selection of metal precursor. In 2019, Cui's group reported the exfoliation of layered crystals prepared from *p-tert*-butylsulfonyl calix[4] arenes capped Zn_4 clusters and 2,2¢-dihydroxyl-1,1¢-binol(biphenol)-3,3¢-dicarboxylic acids.[9] Crystallographic information demonstrates that bulky ligands capped to metal clusters benefit the fabrication of ultrathin nanosheets via weak hydrophobic interactions between interlayers. With these pioneering works in mind, challenges still exist in conceiving feasible design and preparation strategies as well as obtaining high-resolution TEM images.

Cui's group recently supplemented another progression in the preparation of chiral MONs while presenting the first example of high-resolution TEM images of chiral MOFs.[10] The well-defined nanosheets were obtained by exfoliation of three bulk chiral MOFs with new crystal structures. Meanwhile, using the low-dose TEM technique, the ordered pore channels and metal nodes are clearly observed. In detail, (R)- or (S)-6,6¢-dimethyl-5,5¢-di(4-carboxylic acid)phenyl-3,3¢-dimesityl-1,1′-biphenyl-2,2′-dioxaphosphepine as the chiral ligand (Figure 1A) satisfies the coordination requirement with two -COOH, and the rigidity has been well adjusted by the introduction of methyl and mesityl groups. Notably, the weak van der Waals interactions between mesityl groups could connect neighboring layers, which facilitate the exfoliation. Further, the lanthanide(III) metal precursor was chosen for two reasons: (1) serving as a classic coordination node with carboxylic acid, and (2) increasing the structural stability of resultant MOFs that enables high-resolution TEM imaging. Subsequently, three isostructural lanthanide-based MOFs with a formula of $[H_2NMe_2]_2[Ln_2(ligand)_4]$ (Ln = Eu, Dy, and Tb) were prepared. Ultrathin chiral MONs were readily obtained through solvent-assisted liquid sonication thanks to the weak interaction between adjacent layers. Different from the bulk porous MOFs with a diameter of ~50 μm (Figure 1B), the Tyndall effect upon irradiation of the colloid suspensions of MONs confirms the successful exfoliation, and ultrathin and wrinkled 2D nanosheets could also be observed from TEM images (Figure 1C). Utilizing the recently developed low-dose high-resolution TEM, much-improved resolution (<4 Å) of Eu-MOF was achieved (Figure 1D). The high-resolution TEM image based on the contrast transfer function of the objective lens could make it more interpretable. Accordingly, the "black dots," "gray stripes," and "white areas" correspond to the metal clusters, ligands, and channels, respectively (Figures

[1]Department of Chemistry, University of North Texas, Denton, TX 76201, USA

*Correspondence: Shengqian.Ma@unt.edu

https://doi.org/10.1016/j.matt.2021.07.002

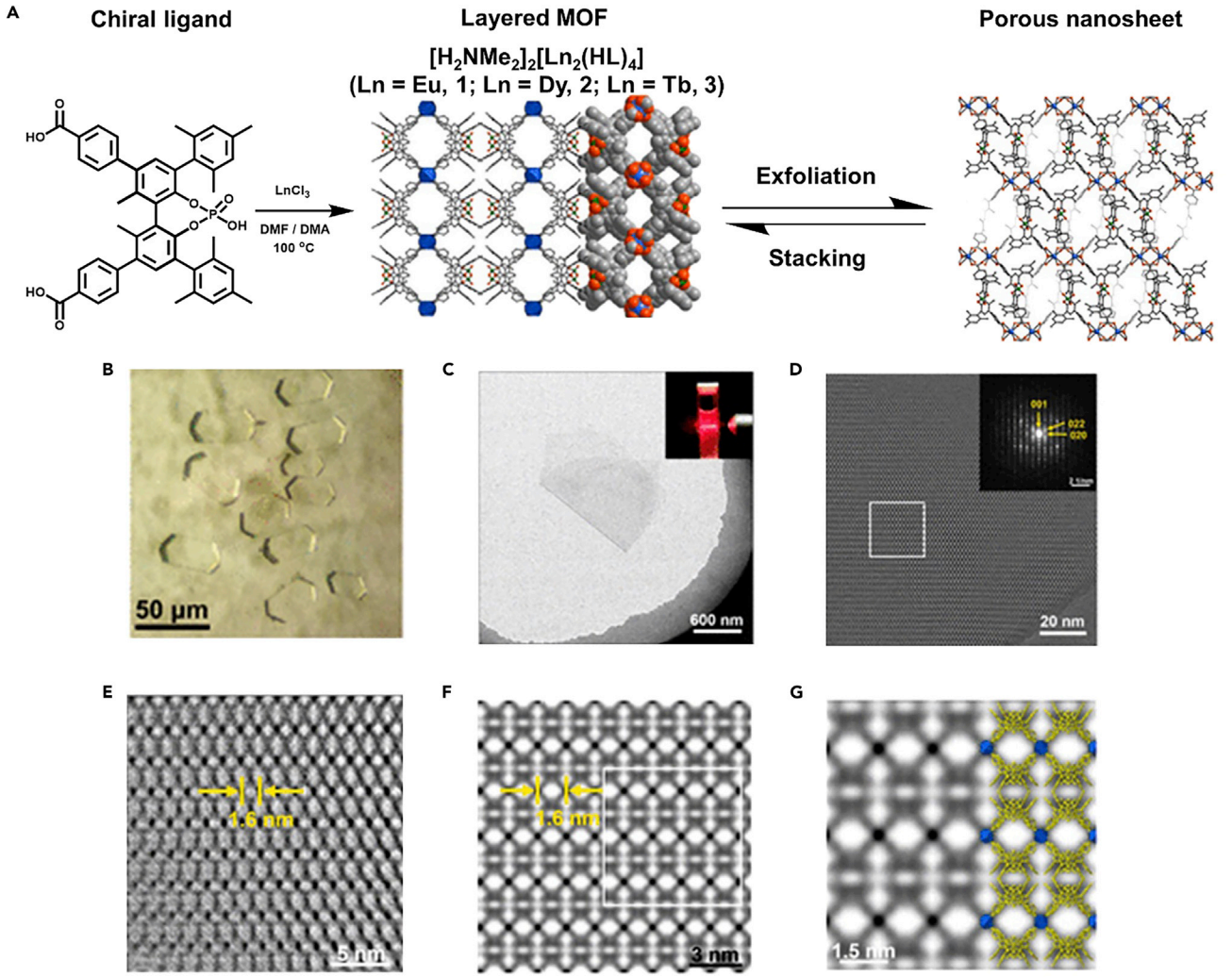

Figure 1. Preparation and characterization of chiral MONs

(A) Scheme for the preparation of chiral MONs.

(B) The microscopic image of the colorless polyhedral crystals (MOF-1).

(C) Regular TEM image of ultrathin chiral Eu-MONs. Inset: photograph of the Tyndall effect of the chiral Eu-MONs suspension.

(D) Low-dose high-resolution motion-corrected TEM image of MOF-1. Inset: the selected area electron diffraction (SAED) pattern of the corresponding crystal.

(E) Contrast transfer function (CTF)-corrected and denoised high-resolution TEM image determined from the white solid lined square in (D).

(F) Simulated projected potential map along the [100] zone axis with point spread function width (PSF) of 3 Å.

(G) Enlarged simulated projected potential map from the white solid lined square in (F), in which the single-crystal structural model is embedded (blue, metal cluster; yellow, ligand).

1E–1G), thus realizing the direct observation of a chiral MOF framework.

It is anticipated that the inspiring work of Cui et al. could allow the chiral MONs to flourish in preparation, characterization, and application. In the aspect of preparation strategy, the few reported examples are still not enough to satisfy the immense demand of chiral materials, including MONs. Similar to various methods utilized in the preparation of nanosheets from bulk porous substrates, there is still plenty of room to afford chiral MONs considering the rarely reported cases. Moreover, the preparation strategy is applicable to diverse porous frameworks, especially crystalline frameworks such as covalent organic frameworks. Meanwhile, the controllable and scalable preparation of chiral MONs for targeted application would be the desirable outcome. From the viewpoint of structural measurement, observing the structure at a smaller scale that provides direct proof for both the coordination mode and coordination environment could be expected with current progress achieved in high-resolution TEM. Otherwise, to distinguish the structural chirality by simply examining the

image is predictable. Furthermore, with the accumulation of experience in observing the structure, we foresee the development of sophisticated instruments to perform direct *in situ* structural modification at the atomic scale. Regarding the application of chiral MONs, enantioseparation of racemic mixtures Δ and tris-oxalatochromium(III) as chiral magnet enantiomers, enantioselective condensation and cyclization of 2-aminobenzamide with aldehydes, and enantioselective fluorescent sensing of a series of functional terpene and terpenoid molecules have been fulfilled with superior performance in different chiral MON systems, and all chiral MONs exhibited better performance than their bulk counterparts. Further applications will be exploited in a boundless chiral world by the utilization of chiral MONs in both chiral small-molecule and macromolecule systems. Within a cycle, the structural characterization confirms the successful preparation of materials and helps to understand how chirality manifests from the MONs to the substrates and, in turn, how the application drives the preparation and characterization of chiral MONs. Therefore, there are still challenges and opportunities in building the connection between MONs and the world of chiral synthesis, separation, and recognition.

ACKNOWLEDGMENTS

This work was supported by the Robert A. Welch Foundation (B-0027).

1. Li, B.Y., Chrzanowski, M., Zhang, Y.M., and Ma, S.Q. (2016). Applications of metal-organic frameworks featuring multi-functional sites. Coord. Chem. Rev. *307*, 106–129.

2. Peng, Y., Li, Y., Ban, Y., Jin, H., Jiao, W., Liu, X., and Yang, W. (2014). Membranes. Metal-organic framework nanosheets as building blocks for molecular sieving membranes. Science *346*, 1356–1359.

3. Zhao, S.L., Wang, Y., Dong, J.C., He, C.T., Yin, H.J., An, P.F., Zhao, K., Zhang, X.F., Gao, C., Zhang, L.J., et al. (2016). Ultrathin metal-organic framework nanosheets for electrocatalytic oxygen evolution. Nat. Energy *1*, 16184.

4. Rodenas, T., Luz, I., Prieto, G., Seoane, B., Miro, H., Corma, A., Kapteijn, F., Llabrés I Xamena, F.X., and Gascon, J. (2015). Metal-organic framework nanosheets in polymer composite materials for gas separation. Nat. Mater. *14*, 48–55.

5. Makiura, R., Motoyama, S., Umemura, Y., Yamanaka, H., Sakata, O., and Kitagawa, H. (2010). Surface nano-architecture of a metal-organic framework. Nat. Mater. *9*, 565–571.

6. Zhao, M., Wang, Y., Ma, Q., Huang, Y., Zhang, X., Ping, J., Zhang, Z., Lu, Q., Yu, Y., Xu, H., et al. (2015). Ultrathin 2D metal-organic framework nanosheets. Adv. Mater. *27*, 7372–7378.

7. Mitra, S., Kandambeth, S., Biswal, B.P., Khayum M, A., Choudhury, C.K., Mehta, M., Kaur, G., Banerjee, S., Prabhune, A., Verma, S., et al. (2016). Self-exfoliated guanidinium-based ionic covalent organic nanosheets (iCONs). J. Am. Chem. Soc. *138*, 2823–2828.

8. Guo, J., Zhang, Y., Zhu, Y., Long, C., Zhao, M., He, M., Zhang, X., Lv, J., Han, B., and Tang, Z. (2018). Ultrathin chiral metal-organic-framework nanosheets for efficient enantioselective separation. Angew. Chem. Int. Ed. Engl. *57*, 6873–6877.

9. Tan, C., Yang, K., Dong, J., Liu, Y., Liu, Y., Jiang, J., and Cui, Y. (2019). Boosting enantioselectivity of chiral organocatalysts with ultrathin two-dimensional metal-organic framework nanosheets. J. Am. Chem. Soc. *141*, 17685–17695.

10. Liu, Y., Liu, L., Chen, X., Liu, Y., Han, Y., and Cui, Y. (2021). Single-crystalline ultrathin 2D porous nanosheets of chiral metal-organic frameworks. J. Am. Chem. Soc. *143*, 3509–3518.

Assessing battery kinetics with machine learning

Rahul Malik[1] and Brandon R. Sutherland[2,*]

The ionic diffusion characteristics of electrode materials critically influence the performance of batteries. Over the last decade, disordered rocksalt materials have emerged as promising next-gen battery cathodes. The higher degree of disorder in these materials results in increased computational complexity when assessing ionic diffusion profiles. Recently in *Electrochimica Acta*, Chang, Jorgensøn and co-authors reported a machine-learning-accelerated method to rapidly evaluate local ionic diffusion barriers in electrode materials with high accuracy.

Key performance metrics of batteries are often directly determined by the fundamental thermodynamic and kinetic properties of their electrode materials. For example, the energy of a lithium-ion cell is defined as the product of the cell voltage, which is related to the Li chemical potential difference between anode and cathode materials, and the capacity, which is related to the available number of redox centers and Li intercalation sites in the electrode materials' crystal structures.

Similarly, if ionic diffusion is sufficiently rapid in a battery's electrode materials, then high input and output cell power may be possible. However, if the Li

[1]CAMX Power LLC, Lexington, MA 02421, USA

[2]A3MD, University of Toronto, Toronto, ON M5S 3G8, Canada

*Correspondence: brandon.sutherland@utoronto.ca

https://doi.org/10.1016/j.matt.2021.07.003